

Giant tunneling magnetoresistance up to 330% at room temperature in sputter deposited Co₂FeAl / MgO / CoFe magnetic tunnel junctions

Wenhong Wang, Hiroaki Sukegawa, Rong Shan, Seiji Mitani, and Koichiro Inomata

Citation: [Applied Physics Letters](#) **95**, 182502 (2009); doi: 10.1063/1.3258069

View online: <http://dx.doi.org/10.1063/1.3258069>

View Table of Contents: <http://scitation.aip.org/content/aip/journal/apl/95/18?ver=pdfcov>

Published by the [AIP Publishing](#)

Articles you may be interested in

[Tunnel magnetoresistance in textured Co₂FeAl / MgO / CoFe magnetic tunnel junctions on a Si / SiO₂ amorphous substrate](#)

Appl. Phys. Lett. **98**, 192505 (2011); 10.1063/1.3587640

[In situ heat treatment of ultrathin MgO layer for giant magnetoresistance ratio with low resistance area product in CoFeB/MgO/CoFeB magnetic tunnel junctions](#)

Appl. Phys. Lett. **93**, 192109 (2008); 10.1063/1.3021372

[Large tunneling magnetoresistance effect at high voltage drop for Co-based Heusler alloy/MgO/CoFe junctions](#)

J. Appl. Phys. **101**, 09J503 (2007); 10.1063/1.2711070

[Tunneling magnetoresistance in \(001\)-oriented Fe Co/Mg O/Fe Co magnetic tunneling junctions grown by sputtering deposition](#)

Appl. Phys. Lett. **88**, 222503 (2006); 10.1063/1.2207835

[Large tunnel magnetoresistance at room temperature with a Co₂FeAl full-Heusler alloy electrode](#)

Appl. Phys. Lett. **86**, 232503 (2005); 10.1063/1.1944893

The image shows the cover of the journal Applied Physics Reviews. It features a white background with an orange header containing the 'AIP Applied Physics Reviews' logo. Below the logo is a diagram of a layered structure. The cover is set against a blue background with a molecular model of a crystal lattice.

NEW Special Topic Sections

NOW ONLINE
Lithium Niobate Properties and Applications:
Reviews of Emerging Trends

AIP | Applied Physics Reviews

Giant tunneling magnetoresistance up to 330% at room temperature in sputter deposited $\text{Co}_2\text{FeAl}/\text{MgO}/\text{CoFe}$ magnetic tunnel junctions

Wenhong Wang,^{a)} Hiroaki Sukegawa, Rong Shan, Seiji Mitani, and Koichiro Inomata
*Magnetic Materials Center, National Institute for Materials Science (NIMS), 1-2-1 Sengen,
 Tsukuba 305-0047, Japan*

(Received 14 June 2009; accepted 12 October 2009; published online 3 November 2009)

Magnetoresistance ratio up to 330% at room temperature (700% at 10 K) has been obtained in a spin-valve-type magnetic tunnel junction (MTJ) consisting of a full-Heusler alloy Co_2FeAl electrode and a MgO tunnel barrier fabricated on a single crystal MgO (001) substrate by sputtering method. The output voltage of the MTJ at one-half of the zero-bias value was found to be as high as 425 mV, which is the largest reported to date in MTJs using Heusler alloy electrodes. The present finding suggests that Co_2FeAl may be one of the most promising candidates for future spintronics devices applications. © 2009 American Institute of Physics. [doi:10.1063/1.3258069]

Magnetic tunnel junctions (MTJs) are devices consisting of two ferromagnetic (FM) electrodes separated by a thin insulator barrier, which show large tunnel magnetoresistance (TMR) due to spin-polarized tunneling.^{1,2} According to Julliere's model,³ the TMR ratios for MTJs can be determined by the tunneling spin polarizations at Fermi level (E_F), P_1 and P_2 of the two FM electrodes, i.e., $\text{TMR} = 2P_1P_2 / (1 - P_1P_2)$. Within this simple model, large TMR ratios result from electrodes with large effective spin-polarization values. Thus, the use of half-metallic ferromagnets,⁴ which have a band gap at the E_F for one spin direction and thus exhibit 100% spin polarization at E_F as electrodes for MTJs is a promising approach for achieving a high TMR ratio.

Co-based full-Heusler alloys with a chemical form of Co_2YZ (Y: transition metal, Z: main group element) have much higher Curie temperatures and most of them have been predicted to be HFMs even at room temperature (RT).⁵⁻⁷ Since the first experimental observation of 16% TMR at RT by Inomata *et al.*⁸ in a MTJ using a $\text{Co}_2\text{Cr}_{0.6}\text{Fe}_{0.4}\text{Al}$ Heusler alloy electrode, the relatively large TMR at RT has been reported in MTJs using different Co-based Heusler alloy electrodes.⁹⁻¹³ In our previous work, we have demonstrated the half-metallicity in Heusler alloy of $\text{Co}_2\text{FeAl}_{0.5}\text{Si}_{0.5}$ (CFAS), which has E_F at the middle of the half-metallic band gap.¹⁴⁻¹⁶ However, all the MTJs consisting of half-metallic Co-based Heusler alloys and a MgO barrier fabricated by sputtering method exhibits a large temperature dependence of TMR, resulting in the maximum TMR of 220% at RT,¹² although a large TMR over 700% can be achieved at a low temperature (LT). Very recently, a huge TMR ratio of 386% at RT (832% at 9 K) was reported in a CFAS/MgO/CFAS MTJ grown using molecular beam epitaxy deposition techniques.¹⁷ Nevertheless, to achieve high TMR ratios by sputtering is of prime importance from a technology point of view, because sputtering is the preferred and established method for industrial applications. Here we provide another Heusler alloy of Co_2FeAl (CFA), which exhibits giant TMR ratio as high as 330% at RT in CFA/MgO/CoFe-MTJs fabricated using simple sputter-deposition techniques.

The MTJs with a structure of MgO(001) substrate/Cr(40) / Co_2FeAl (30) / MgO(1.2–2.5) / $\text{Co}_{75}\text{Fe}_{25}$ (5) /

$\text{Ir}_{80}\text{Mn}_{20}$ (12)/Ru(7) (unit: nanometer) was fabricated using an ultrahigh vacuum magnetron sputtering system with the base pressure of below 8×10^{-8} Pa. The bottom CFA electrode was deposited at RT from a stoichiometric Co–Fe–Al (Co: 50.0%, Fe: 25.0%, and Al: 25.0%) target. The Ar pressure during sputtering was 1.0 mTorr and typical deposition rate was 2×10^{-2} nm/s for CFA. We found that the as-deposited CFA film composition was $\text{Co}_{52.8}\text{Fe}_{25.4}\text{Al}_{21.8}$ through inductively coupled plasma analysis. The film was subsequently annealed at 480 °C for 15 min in order to improve the quality. The crystal structures were characterized by x-ray diffraction (XRD). Surface morphology and surface roughness were investigated using atomic force microscopy (AFM). We also tried other conditions with various annealing temperatures for the bottom CFA electrode, but the above-mentioned condition yielded the highest TMR ratio. The MgO tunnel barrier was formed by rf sputtering directly from a sintered MgO target under an Ar pressure of 10 mTorr. The MTJs were patterned into an area of $10 \times 10 \mu\text{m}^2$ using conventional photolithography and Ar ion milling process. Patterned MTJs were annealed at T_a from 300 to 475 °C for 1 h in high vacuum by applying a 5 kOe magnetic field. Magnetoresistance measurements were carried out using the standard dc four-point probe method from 7 to 300 K. In this study, the magnetic field was applied along in the plane and the positive current is defined as that electrons flow from the top CoFe layer to the bottom CFA layer.

Figure 1 shows x-ray θ -2 θ diffraction pattern of CFA bottom layer after *in situ* annealing at 480 °C. In addition to peaks from MgO substrate, only the (002) Cr peak and (002) and (004) CFA peaks were detected, indicating that the CFA film grows with almost perfect (001) orientation on Cr-buffered MgO (001) surface. The appearance of (002) superlattice line reveals mostly the B2-ordered structure for the CFA film deposited on Cr-buffered MgO (001) substrate at RT and subsequently annealed at 480 °C. The inset (a) of Fig. 1 shows the XRD pole figure of B2 (222) superlattice line for the CFA film. The clear (222) peaks with the fourfold symmetry further indicate that the 480 °C annealed CFA film is epitaxial and single-crystalline film. $L2_1$ (111) could not be observed, which implies the existence of complete disorder between Fe and Al, while Co atoms occupy regular

^{a)}Electronic mail: w_wenhong@yahoo.com.

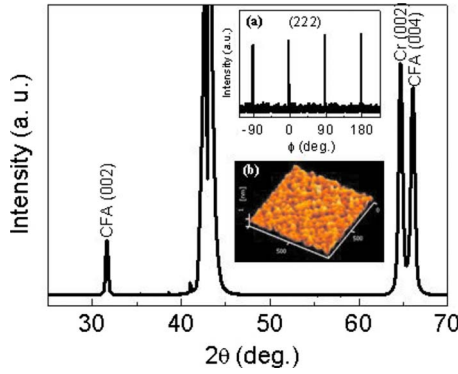


FIG. 1. (Color online) XRD pattern of MgO (001) substrate/Cr (40 nm)/Co₂FeAl (30 nm) after *in situ* annealing at 480 °C. Inset (a) shows ϕ -scan measurement of the (222) plane of Co₂FeAl film. The surface morphology of Co₂FeAl as observed by AFM is shown in inset (b).

sites. We should note that the degree of spin polarization predicted for the $L2_1$ structure is conserved for $B2$ ordered CFA,¹⁸ thus one might expect high TMR ratios in MTJs with CFA electrodes. Moreover, the surface morphology observed by AFM was extremely flat, as shown in inset (b) of Fig. 1. An average surface roughness (R_a) of 0.2 nm was achieved for the 480 °C annealed CFA film. This result suggests that the 480 °C annealed CFA film is suitable for stacking a MTJ structure.

Figure 2 shows TMR ratios measured at RT as a function of postannealing temperature (T_a) for the CFA/MgO/CoFe-MTJ with MgO thickness (t_{MgO}) of 1.8 nm. It was found that the TMR ratio increases with increasing T_a and reaches its maximum value of 330% at $T_a=450$ °C. The inset shows the typical TMR curves of the MTJ annealed at $T_a=300$ and 450 °C, respectively. We should point out that the highest TMR ratio was observed at $t_{\text{MgO}}=1.8$ nm, while giant TMR ratios above 280% were obtained in a wide range of t_{MgO} from 1.5 to 2.5 nm. Obviously, these TMR ratios of CFA/MgO/CoFe-MTJs are much higher than that of Co₂Cr_{0.6}Fe_{0.4}Al/MgO/CoFe MTJs (109% at RT)¹³ and Co₂MnSi/MgO/CoFe MTJs (217% at RT),¹⁹ suggesting that the $B2$ -ordered CFA electrode is effective in enhancing the TMR effect. The increase in TMR with the annealing process is probably due to the improvement of both interface structure and (001) orientation of the MgO barrier. While, the TMR ratio starts to decrease at T_a higher than 450 °C, which

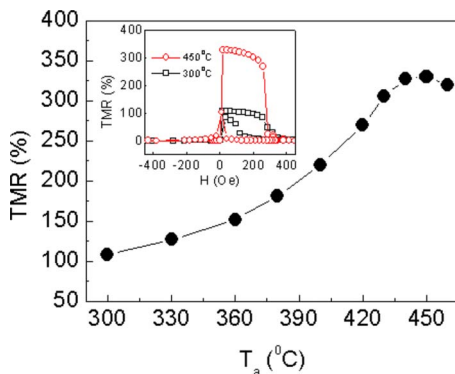


FIG. 2. (Color online) Annealing temperature (T_a) dependence of the RT TMR ratio of the CFA/MgO/CoFe-MTJ with MgO thickness of 1.8 nm. The inset shows the typical MR curves at 300 and 450 °C, respectively. All measurements were conducted at RT under an applied bias voltage of +1 mV.

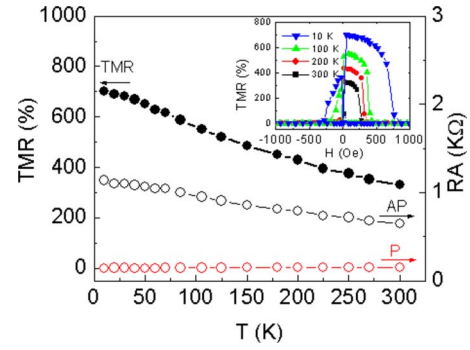


FIG. 3. (Color online) Measured temperature dependences of both TMR ratio and resistance area (RA) product for parallel (p) and antiparallel (AP) magnetization configurations for the CFA/MgO/CoFe-MTJ annealed at $T_a=450$ °C. The inset shows the MR curves measured at 10, 100, 200, and 300 K, respectively. All measurements were conducted under an applied bias voltage of +1 mV.

can be understood as being due to the interdiffusion of Mn from antiferromagnetic IrMn layer to the MgO tunnel barrier. Thus, a possible scenario of achieving a higher TMR ratio at high T_a is to use synthetic FM pinned layer as confirmed in the MTJs with CoFeB electrodes.²⁰

Figure 3 shows the temperature dependence of TMR ratio and RA (resistance area product) of the P and AP states of the MTJ annealed at $T_a=450$ °C. The TMR curves measured at various temperatures are shown in the inset of Fig. 3. The TMR ratio of the CFA/MgO/CoFe-MTJ increased gradually with decreasing temperature, and a huge TMR ratio of 700% was observed at 10 K. Thus, the ratio of TMR between LT and RT, $\text{TMR}(10\text{ K})/\text{TMR}(300\text{ K})$, for the CFA/MgO/CoFe-MTJ is 2.1. This is a very small temperature variation in TMR ratio compared with that in the other Heusler alloys MTJs. In a fully epitaxial Co₂MnSi/MgO/CoFe MTJ,¹⁹ for example, the ratio of $\text{TMR}(\text{LT})/\text{TMR}(\text{RT})$ is found to be 3.5. It is worthy to note that a small temperature variation in TMR ratio is desirable for practical spintronics device applications. The resistance in the AP configuration gradually increases as temperature decreases, while that in the P configuration remains almost constant. This result suggests that the temperature dependence of the TMR ratio is mainly determined by that of RA in the AP state, which is a commonly observed feature of MgO-based MTJs.^{10,21}

Now we would like to discuss the origin of the huge TMR effect observed in CFA/MgO/CoFe-MTJs. The Jullière's model is often used to relate TMR with tunneling spin polarization at E_F of the FM electrodes. However, a straightforward application of this model for a TMR ratio of 330% at RT for the CFA/MgO/CoFe-MTJ with a CoFe electrode spin polarization of 0.50, results in an unrealistically high spin-polarization value exceeding 1.0 for the $B2$ -ordered CFA electrode. This result indicates enhancement in the TMR ratio by a coherent tunneling contribution²² for CFA/MgO/CoFe-MTJs, although a detailed theoretical calculation will be required in future.

Figure 4 shows the normalized TMR ratio (open circle) and output voltage [$V_{\text{out}}=V_p \times (R_{\text{ap}}-R_p)/R_{\text{ap}}$, solid circle] as functions of bias voltage V . The TMR ratio was found to decrease with increasing bias voltage, and a slight asymmetry was observed for positive and negative bias voltages, which is due to the difference of the bottom CFAS/MgO and top MgO/CoFe interfaces. The TMR ratios dropped to one-

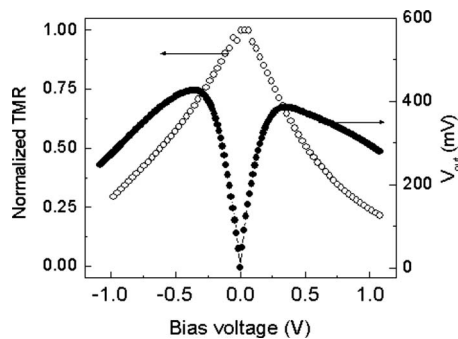


FIG. 4. Normalized TMR ratio (open circles) and output voltage V_{out} (filled circles), defined as $V_{\text{out}} = V_p \times (R_{\text{ap}} - R_p) / R_{\text{ap}}$, as a function of bias voltage V for the CFA/MgO/CoFe-MTJ. Bias voltage where TMR ratio becomes one-half of zero-bias value is 500 mV for positive and 600 mV for negative bias directions. Maximum V_{out} shows about 425 mV.

half of the zero-bias value (V_{half}) at about 500 and 600 mV for positive and negative bias voltages, respectively. The maximum output voltage is about 425 and 380 mV for the negative and positive bias, respectively. It is worthy to note that the output signal is the highest reported to date in MTJs using Heusler alloy electrodes,^{9–17} and comparable with that of fully epitaxial Fe/MgO/Fe²³ and CoFeB/MgO/CoFeB²⁴ MTJs, when compared at the same bias voltage.

In summary, we have fabricated the fully epitaxial MTJs using the highly *B2*-ordered CFA electrode and a MgO tunnel barrier on a MgO (001) substrate using simple sputter-deposition techniques. The microfabricated MTJ exhibits a very high MR ratio of 330% and the maximum V_{out} 425 mV at RT. The giant TMR and high output signal of these MTJs structure, together with the low damping constant of Heusler alloy Co₂FeAl,²⁵ suggest that this material may play a key role in future spintronics devices operating at RT.

This work was partly supported by the NEDO, CREST, and JST-DFG (FE633/6–1).

¹J. S. Moodera, L. R. Kinder, T. M. Wong, and R. Meservy, *Phys. Rev. Lett.* **74**, 3273 (1995).

- ²T. Miyazaki and N. Tezuka, *J. Magn. Magn. Mater.* **139**, L231 (1995).
- ³M. Julliere, *Phys. Lett. A* **54**, 225 (1975).
- ⁴R. A. de Groot, F. M. Mueller, P. G. van Engen, and K. H. J. Buschow, *Phys. Rev. Lett.* **50**, 2024 (1983).
- ⁵S. Ishida, S. Fujii, S. Kashiwagi, and S. Asano, *J. Phys. Soc. Jpn.* **64**, 2152 (1995).
- ⁶I. Galanakis, P. H. Dederichs, and N. Papanikolaou, *Phys. Rev. B* **66**, 174429 (2002).
- ⁷S. Picozzi, A. Continenza, and A. J. Freeman, *Phys. Rev. B* **66**, 094421 (2002).
- ⁸K. Inomata, S. Okamura, R. Goto, and N. Tezuka, *Jpn. J. Appl. Phys., Part 2* **42**, L419 (2003).
- ⁹Y. Sakuraba, M. Hattori, M. Oogane, Y. Ando, H. Kato, A. Sakuma, T. Miyazaki, and H. Kubota, *Appl. Phys. Lett.* **88**, 022503 (2006).
- ¹⁰T. Ishikawa, T. Marukame, H. Kijima, K.-I. Matsuda, T. Uemura, M. Arita, and M. Yamamoto, *Appl. Phys. Lett.* **89**, 192505 (2006).
- ¹¹T. Ishikawa, S. Hakamata, K.-I. Matsuda, T. Uemura, and M. Yamamoto, *J. Appl. Phys.* **103**, 07A919 (2008).
- ¹²S. Okamura, A. Miyazaki, S. Sugimoto, N. Tezuka, and K. Inomata, *Appl. Phys. Lett.* **86**, 232503 (2005).
- ¹³T. Marukame, T. Ishikawa, S. Hakamata, K. Matsuda, T. Uemura, and M. Yamamoto, *Appl. Phys. Lett.* **90**, 012508 (2007).
- ¹⁴W. H. Wang, H. Sukegawa, R. Shan, T. Furubayashi, and K. Inomata, *Appl. Phys. Lett.* **92**, 221912 (2008).
- ¹⁵H. Sukegawa, W. H. Wang, R. Shan, T. Nakatani, K. Inomata, and K. Hono, *Phys. Rev. B* **79**, 184418 (2009).
- ¹⁶R. Shan, H. Sukegawa, W. H. Wang, M. Kodzuka, W. F. Li, T. Furubayashi, S. Mitani, K. Inomata, and K. Hono, *Phys. Rev. Lett.* **102**, 246601 (2009).
- ¹⁷N. Tezuka, N. Ikeda, F. Mitsuhashi, and S. Sugimoto, *Appl. Phys. Lett.* **94**, 162504 (2009).
- ¹⁸S. Wurmehl, J. T. Kohlhepp, H. J. M. Swagten, and B. Koopmans, *J. Phys. D: Appl. Phys.* **41**, 115007 (2008).
- ¹⁹S. Tsunegi, Y. Sakuraba, M. Oogane, K. Takanashi, and Y. Ando, *Appl. Phys. Lett.* **93**, 112506 (2008).
- ²⁰Y. M. Lee, J. Hayakawa, S. Ikeda, F. Matsukura, and H. Ohno, *Appl. Phys. Lett.* **89**, 042506 (2006).
- ²¹S. S. P. Parkin, C. Kaiser, A. Panchula, P. M. Rice, B. Hughes, M. Samant, and S.-H. Yang, *Nature Mater.* **3**, 862 (2004).
- ²²W. H. Butler, X.-G. Zhang, T. C. Schulthess, and J. M. MacLaren, *Phys. Rev. B* **63**, 054416 (2001).
- ²³S. Yuasa, T. Nagahama, A. Fukushima, Y. Suzuki, and K. Ando, *Nature Mater.* **3**, 868 (2004).
- ²⁴D. D. Djayaprawira, K. Tsunekawa, M. Nagai, H. Maehara, S. Yamagata, N. Watanabe, S. Yuasa, Y. Suzuki, and K. Ando, *Appl. Phys. Lett.* **86**, 092502 (2005).
- ²⁵S. Mizukami, D. Watanabe, M. Oogane, Y. Ando, Y. Miura, M. Shirai, and T. Miyazaki, *J. Appl. Phys.* **105**, 07D306 (2009).